

Continuous-wave-controlled nonlinear x-wave generation

Yannis Kominis, Nikolaos Moshonas, Panagiotis Papagiannis, and Kyriakos Hizanidis

School of Electrical and Computer Engineering, National Technical University of Athens, 157 73 Athens, Greece

Demetrios N. Christodoulides

College of Optics—Center for Research and Education in Optics and Lasers, University of Central Florida, Orlando, Florida 32816-2700

Received June 7, 2005; accepted June 29, 2005

We demonstrate that the interaction between a two-dimensional localized wave packet and a continuous-wave background can lead to efficient x-wave generation in nonlinear bidispersive optical systems. This x-wave generation process was found to depend on both the relative phase and amplitude of the background with respect to the superimposed wave packet. Pertinent configurations that lead to such generation are considered. © 2005 Optical Society of America

OCIS codes: 190.7110, 190.3270, 050.1940, 320.7120, 320.5550.

In the past few years, nonlinear x-wave generation has been a subject of intense investigation.^{1–3} Three-dimensional x waves were suggested and observed by Lu and Greenleaf within the context of ultrasonics⁴ and were subsequently realized in linear optics by use of so-called holographic lensacon techniques.⁵ In general, the formation of this class of wave results from the linear bidispersive properties of the underlying system and can occur in both the linear and the nonlinear domains. In nonlinear optics, 3D spatiotemporal x-wave structures have been observed in normally dispersive lithium triborate $\chi^{(2)}$ crystals¹ and in water cells,^{6,7} and also have been theoretically analyzed in both quadratic and Kerr nonlinear media.² A major issue concerning x-wave generation is the efficiency with which these waves can be nonlinearly excited. As was recently noted by Di Trapani, nonlinear x-wave formation in three dimensions (in space–time) is typically associated with the halos of a spatiotemporal pulse (which induce it) and is therefore rather weak.⁸ Part of the reason for such low efficiency is the fact that the induced weak conical dispersive wave related to the x component is distributed over three dimensions. In addition, the x-wave linear solutions are by their nature infinite energy entities,^{4,9} and thus realistically only x-like structures can be expected in any experimental situation.

Recently the existence of 2D linear x waves was theoretically demonstrated,⁹ and the excitation of discrete x-like spatiotemporal structures in nonlinear normally dispersive waveguide arrays has also been considered.¹⁰ In Ref. 9 the possibility of using the linear interference between a continuous background and a Gaussian beam to generate dispersive x-like structures was suggested as an alternative to previously used techniques that require nontrivial beam shaping. Clearly, it will be of great interest to develop new approaches through which x waves can be efficiently and spontaneously generated from nonlinearity in a more sustainable fashion. In the nonlinear regime such x waves are expected to exhibit stronger

localization through self-focusing and a much richer dynamic behavior.

In this Letter we show that the nonlinear interaction between a 2D localized wave packet and a continuous-wave (cw) background can lead to efficient x-wave generation in bidispersive optical systems. We found that this process depends strongly on both the amplitude and the relative phase of the cw background with respect to the superimposed wave packet. Unlike what happens in the anomalous dispersion regime,¹¹ the nonlinear mechanism responsible for the generated x-wave structure is due to cw-seeded modulational instability¹² and self-focusing effects. The possibility of cw-controlled generation of spatiotemporal x-waves in normally dispersive nonlinear planar waveguides is discussed by means of relevant examples.

To analyze cw-controlled x-wave generation, let us consider for example a Kerr nonlinear planar normally dispersive waveguide. In this case the underlying spatiotemporal evolution problem is described by a (2+1)*D* nonlinear Schrödinger equation:

$$i \frac{\partial U}{\partial z} + \frac{\partial^2 U}{\partial X^2} - \frac{\partial^2 U}{\partial T^2} + |U|^2 U = 0, \quad (1)$$

where $Z = z/z_0$, $X = x/x_0$, and $T = (t - zv_g^{-1})/t_0$ are the normalized longitudinal, transverse, and time coordi-

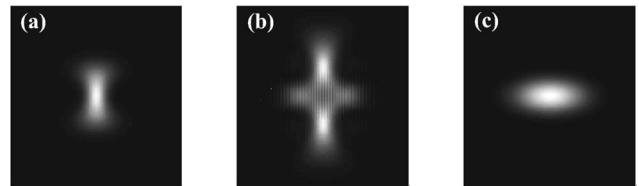


Fig. 1. Output intensity profile resulting from a Gaussian wave packet at $z = 15$ mm ($Z = 5$) when $t_{\text{FWHM}} = 112$ fs ($\rho = 1/3$): (a) $I_{\text{max}} = 15$ W/ μm^2 ($A^2 = 8/3$, $E = 2E_{\text{cr}}$), (b) $I_{\text{max}} = 30$ W/ μm^2 ($A^2 = 16/3$, $E = 4E_{\text{cr}}$), and (c) under linear conditions. Vertical and horizontal axes, respectively, depict the time interval ($t = -1.35$ – 1.35 ps) and the transverse coordinate ($x = -315$ – 315 μm).

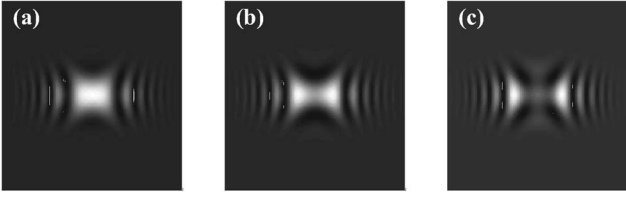


Fig. 2. Output intensity profile resulting from a Gaussian wave packet at $z=15$ mm ($Z=5$) when $t_{\text{FWHM}}=112$ fs ($\rho=1/3$) and $I_{\text{max}}=15$ W/ μm^2 ($A^2=8/3$, $E=2E_{\text{cr}}$), in the presence of a cw with $B=0.1$ A and phase φ of (a) 0, (b) $\pi/2$, and (c) π in a linear medium. Vertical and horizontal axes, respectively, depict the time interval ($t=-1.35-1.35$ ps) and the transverse coordinate ($x=-315-315$ μm).

nates, respectively, and v_g is the group velocity. U is a normalized electric field Q envelope amplitude, which is given by $U=Q/I_0^{1/2}$, where I_0 is a characteristic intensity. For illustration purposes we assume here that the planar waveguide is made from AlGaAs that has the following parameters at $\lambda_0=1.55$ μm : The linear refractive index is $n=3.34$, the nonlinear Kerr coefficient is $n_2=1.5 \times 10^{-13}$ cm^2/W , and its normal dispersion is $k''=1.35 \times 10^{-24}$ $\text{s}^2 \text{m}^{-1}$. If the reference width in the x direction is $x_0=10.5$ μm , we get $z_0=3$ mm, $t_0=45$ fs, and $I_0=5.5$ W/ μm^2 . The effective transverse width of this waveguide is taken here to be 1 μm , and its length is $z=15$ mm (or $Z=5$). In numerically solving Eq. (1) we utilized a split-step Fourier method. In all cases the spatiotemporal window has been taken as broad enough to prevent artificial reflections from the boundaries, and the accuracy was monitored by use of the conserved quantities of Eq. (1). Equation (1) is also used to describe propagation of nonlinear beams in bidiffractive lattices.⁹

It is important to note that the bidispersive character of Eq. (1) prevents any collapse from occurring; instead, it leads to pulse splitting.¹³⁻¹⁵ Had the dispersion been anomalous, the critical normalized energy $E_{\text{cr}}=\iint |U|^2 dX dT$ necessary for catastrophic collapse would have been (for a Gaussian beam input) 4π ,¹⁶ and, as a matter of fact, we use this level as a norm in our study.

To investigate nonlinear x-wave generation in such a bidispersive system we assume at the input ($Z=0$) a coherent superposition of an elliptical spatiotemporal Gaussian wave packet of the form $u_{\text{wp}}=A \exp[-(X^2+\rho^2 T^2)/2]$ with a broad cw described by $u_{\text{cw}}=B \exp(i\varphi)$, where A and ρ represent the amplitude and the spatiotemporal ellipticity of the beam and B and φ are the amplitude and the relative phase difference (relative to the wave packet) of the background, respectively. Both the cw and the Gaussian wave packet are coherent with respect to each other and exhibit the same frequency and polarization. In all cases we assume that the ellipticity parameter of the Gaussian wave packet is $\rho=1/3$. According to the normalizations adopted above, this corresponds to a FWHM pulse duration of 112 fs and a beam width of 10.5 μm .

We first investigate the dynamics of the Gaussian wave packet in the absence of a cw background under nonlinear and linear conditions. Fig. 1 shows the in-

tensity of the wave packet at the output of the AlGaAs waveguide ($z=1.5$ cm) for various peak power-density levels. As Fig. 1(a) demonstrates, the x-wave formation is in this case (for a peak power $P_{\text{max}} \approx 270$ W) weak and is embedded in the halo of the pulse. At higher intensities ($P_{\text{max}} \approx 550$ W), the packet undergoes pulse splitting, as shown in Fig. 1(b). Note that, in the linear regime (very low powers), the wave packet would have spread as an elliptic Gaussian because of bidispersion [see Fig. 1(c)].

We next consider how the cw background affects the dispersion-diffraction linear dynamics of this wave packet as a function of relative phase φ . Figure 2 depicts this evolution when $B/A=0.1$ and for $\varphi=0, \pi/2, \pi$. In this case a dispersive x-like structure is formed, thus indicating that the presence of a cw is essential.⁹ Depending on the initial phase difference, the intensity escapes from the center of the pattern and disperses along hyperbolic branches. Yet because of dispersion these x-like structures are not strongly localized and are short lived.

Figure 3 shows nonlinearly induced x-wave generation in the presence of a constant background when $B/A=0.1, 0.3, 0.5$ and for $\varphi=0, \pi/2, \pi$. In all cases depicted in Fig. 3, the wave packet's peak power is $P_{\text{max}} \approx 270$ W. As in the linear regime, this process depends crucially on both the intensity ratio and relative phase φ . Our results indicate that x-wave formation happens to be more efficient when the two components are out of phase, especially when $\varphi \approx \pi/2$ [see, for example, Figs. 3(b), 3(e), and 3(h)], in which case the intensity peaks at the center. In these cases we have found that x waves are stably gener-

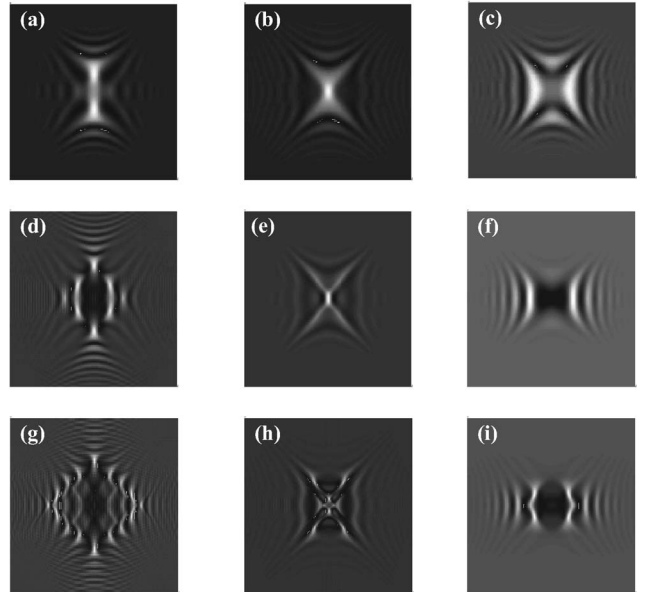


Fig. 3. Output intensity profile resulting from a Gaussian wave packet at $z=15$ mm ($Z=5$) when $t_{\text{FWHM}}=112$ fs ($\rho=1/3$) and $I_{\text{max}}=15$ W/ μm^2 ($A^2=8/3$, $E=2E_{\text{cr}}$), in the presence of a cw with (a)–(c) $B=0.1$ A, (d)–(f) $B=0.3$ A, (g)–(i) $B=0.5$ A; and (a), (d), (g) $\varphi=0$; (b), (e), (h) $\pi/2$; and (c), (f), (i) π in a nonlinear medium. Vertical and horizontal axes, respectively, depict the time interval ($t=-1.35-1.35$ ps) and transverse coordinate ($x=-315-315$ μm).

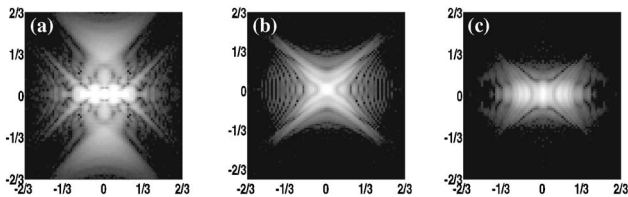


Fig. 4. Output power spectra corresponding to the conditions shown in Figs. 3(d)–3(f). Frequency Ω (vertical axis) and transverse wave number K_X (horizontal axis) are given in normalized units; $\Omega_0 = 2\pi/t_0 \approx 140$ THz and $K_0 = 2\pi/x_0 \approx 0.6 \mu\text{m}^{-1}$.

ated, in the sense that they are always produced and sustained at distances as large as 50 mm. When the two waves are in antiphase ($\varphi = \pi$), the intensity becomes mostly localized on hyperboliclike curves, thus leaving the center devoid of energy. For $\varphi \approx 0$, on the other hand, pulse splitting occurs, while x-wave formation competes with pulse splitting or intensity localization for values of φ in the intervals $(0, \pi/2)$ and $(\pi/2, \pi)$, respectively. In all cases the x structures happen to be more confined in space–time and tend to persist in comparison with the linear conditions examined in Fig. 2. The combined action of bidispersion and nonlinearity depends on the initial conditions. The initial phase difference between the wave packet and the cw background determines the symmetry and the location of the emerging intensity peaks of the emerging patterns, as shown in Fig. 3. The spectral content of these structures [corresponding to Figs. 3(d)–3(f)] is shown in Fig. 4. The initial phase difference results in a spectrum rearrangement along different families of hyperbolas of the linear dispersion relation. A zero phase difference broadens the spectrum along the frequency direction (Ω), while a $\pi/2$ phase difference results in equal spectral widths with respect to both frequency (Ω) and transverse wave number (K_X). In contrast, a π phase difference results in a spectrum that is more extended along the K_X direction.

In conclusion, we have shown that the nonlinear interaction between a 2D localized wave packet and a

continuous-wave background can lead to efficient x-wave generation in bidispersive optical systems. In closing, we note that the processes considered in this Letter are also expected to appear in other nonlinear systems such as those that involve saturable nonlinearities.

This work is supported by grants “Herakleitos” and “Pythagoras” of the Hellenic Ministry of Education and by the U.S. National Science Foundation. K. Hizanidis’s e-mail address is kyriakos@central.ntua.gr.

References

1. P. Di Trapani, G. Valiulis, A. Piskarskas, O. Jedrkiewicz, J. Trull, C. Conti, and S. Trillo, *Phys. Rev. Lett.* **91**, 093904 (2003).
2. C. Conti, S. Trillo, P. Di Trapani, G. Valiulis, A. Piskarskas, O. Jedrkiewicz, and J. Trull, *Phys. Rev. Lett.* **90**, 170406 (2003).
3. J. Trull, O. Jedrkiewicz, P. Di Trapani, A. Matijosius, A. Varanavicius, G. Valiulis, R. Danielius, E. Kucinskas, A. Piskarskas, and S. Trillo, *Phys. Rev. E* **69**, 026607 (2004).
4. J. Y. Lu and J. F. Greenleaf, *IEEE Trans. Ultrason. Ferroelectr. Freq. Control* **39**, 19 (1992).
5. H. Sonajal, M. Ratsep, and P. Saari, *Opt. Lett.* **22**, 310 (1997).
6. A. Dubietis, G. Tamosauskas, I. Diomin, and A. Varanavicius, *Opt. Lett.* **28**, 1269 (2003).
7. M. Kolesik, E. M. Wright, and J. V. Moloney, *Phys. Rev. Lett.* **92**, 253901 (2004).
8. P. Di Trapani, *Phys. Today* **57**(10), 25 (2004).
9. D. N. Christodoulides, N. K. Efremidis, P. Di Trapani, and B. A. Malomed, *Opt. Lett.* **29**, 1446 (2004).
10. S. Droulias, K. Hizanidis, J. Meier, and D. N. Christodoulides, *Opt. Express* **13**, 1827 (2005).
11. Y. Kominis and K. Hizanidis, *J. Opt. Soc. Am. B* **22**, 1360 (2005).
12. L. W. Liou, X. D. Cao, C. J. McKinstrie, and G. P. Agrawal, *Phys. Rev. A* **46**, 4202 (1992).
13. J. E. Rothenberg, *Opt. Lett.* **17**, 583 (1992).
14. G. G. Luther, A. C. Newell, J. V. Moloney, and E. M. Wright, *Opt. Lett.* **19**, 789 (1994).
15. J. K. Ranka, R. W. Schirmer, and A. L. Gaeta, *Phys. Rev. Lett.* **77**, 3783 (1996).
16. M. Desaix, D. Anderson, and M. Lisak, *J. Opt. Soc. Am. B* **8**, 2082 (1991).